Journal of Applied Research and Technology

www.jart.icat.unam.mx

Journal of Applied Research and Technology 21 (2023) 227-240

Original

Master-slave synchronization in the van der Pol and Duffing systems via elastic, dissipative and a combination of both couplings

U. Uriostegui-Legorreta • E. S. Tututi*

Facultad de Ciencias Físico Matemáticas UMSNH, Morelia, México.

Received 07 01 2021; accepted 03 29 2022
Available 04 30 2023

Abstract: A modified master-slave scheme to look for synchronization, based on a general combination of elastic and dissipative couplings, is presented. We focus on solutions according the scheme presented, illustrating the method we use, by employing the van der Pol and Duffing oscillators and analyzing three types of couplings. We find synchronization in the oscillators for large values of the coupling. Nevertheless, no synchronization exists for an elastic coupling, while for the dissipative coupling, we found partial synchronization. For the general combination we obtained complete synchronization.

Keywords: Nonlinear dynamics, control of chaos, synchronization

*Corresponding author.
E-mail address: eduardo.tututi@umich.mx (E. S. Tututi).
Peer Review under the responsibility of Universidad Nacional Autónoma de México.

1. Introduction

Since the seminal work of Pecora and Carrol on synchronization Pecora and Carroll (1990), works on chaos that comprise diverse areas such as lasers, chemical reactions, electronic circuits, biological systems, among others. In particular, low-dimensionality systems have been of interest in order to understand the synchronization and chaotic behavior in nature. The most studied and representative systems are the Lorenz, Chua, Rössler, van der Pol and Duffing ones Chua et al. (1993), Ding and Yang (1996), Lee et al. (1998), Pastor-Díaz and López-Fraguas, (1995), Reick and Mosekilde, (1995), Yin and Dai (1998).

The van der Pol and Duffing oscillators are the paradigmatic circuits to study chaos in systems of low-dimensionality. The first gives a limit cycle and the last provides the prototype of a strange attractor. Studies focused on the van der Pol oscillator revel that it possess a rich dynamical structure, especially when the oscillator is forced. This system exhibits complex bifurcation structures with an important number of periodic states, a chaotic region and islands of periodic states, showing, in addition, transitions from chaos to stable states. The dynamics based on identical or distinct nonlinear oscillators presenting the same kind of attractors is still under study Dongmo et al. (2018), Kuznetsov and Roman (2009), López-Mancilla et al. (2019). Nevertheless, the dynamics of these systems in states of different attractors is of current interest and it could give rise to important information.

The control of chaos is concerned with using some designed control to modify the characteristics of a nonlinear system. A number of methods such as active control, adaptive control, optimal control and sliding mode control exist for the control of chaos in systems Chekan et al. (2017), Huang and Cao (2017), Pai (2020), Ye et al. (2018). Various kinds of synchronization play a very important role such as phase synchronization, anticipated synchronization, generalized synchronization, projective synchronization, complete synchronization, hybrid synchronization, anti-synchronization, multimodal synchronization, forced synchronization, itinerary synchronization and hybrid function projective synchronization have been developed and are frequently used Anzo-Hernández et al. (2019), Campos et al. (2004), Gonzalez-Salas et al. (2008), Khan and Shikha (2017), Ouannas et al. (2017), Razminia and Dumitru (2013), Yan and Li (2005).

Some applications of the van der Pol and Duffing oscillators go from physics to biology, electronics, chemistry and many other fields. For instance, a possible application of synchronization in chaotic signal is to implement secure communication systems. Since chaotic signals are usually broadband, noise like, and difficult to predict the behavior and the information the systems transport. They can also be used for masking information bearing waveforms Lu et al. (2019), Murali and Lakshmanan (1993), Njah (2010). In robotics, the oscillators have been included to control joint hips and knees of human-like robots to ensure the mechanical system follows the right path. The generated signals can be used as reference trajectories for the feedback control Dutra (2003), Jasni and Shafie (2012). Other application is in artificial intelligence. In fact, the oscillators have shown usefulness to training neural network and recognition of chaotic systems Chaharborj et al. (2021), Mall and Chakraverty (2016).

As far as the coupling between the van der Pol and Duffing oscillators is referred, we can mention three different couplings, namely: gyroscopic, dissipative, and elastic Chedjou et al. (2001, 2006), Kuznetsov et al. (2009), Siewe et al. (2010a), Uriostegui-Legorreta et al. (2021), Vicent and Kenfack (2008). Among the diverse ways of coupling, the most used are the elastic and dissipative ones Kengne et al. (2012; 2014). In a previous work Uriostegui-Legorreta et al. (2021), it is analyzed a different approach of synchronizing two distinct oscillators of low dimensionality, using the aforementioned couplings.

In this work, we study and compare three types of couplings by using the van der Pol and Duffing systems: the elastic, the dissipative and a combination of both couplings Uriostegui-Legorreta et al. (2021). It is important to remark that the studies in the literature on this kind of synchronization are based only on one coupling. An outline of this work is as follows. In Sec. 2, it is briefly studied the features of the van der Pol and Duffing oscillators. In Sec. 3, we study and compare three types of couplings using the van der Pol and Duffing systems upon the master-slave configuration. In Sec. 4, some conclusions and an outlook are presented.

2. The systems

As a dynamical system, the van der Pol oscillator is one with nonlinear damping. The time evolution is governed by

$$\ddot{x} - \mu(1 - x^2)\dot{x} + \frac{dU_2(x)}{dx} = A_2 \cos(\omega_2 t), \tag{1}$$

where, as usual, the variable x is real and denotes the position, t the time, and $\mu > 0$ is a parameter that governs the nonlinearity and damping. The external forcing is given by the harmonic function, with amplitude A_2 and frequency ω_2. We have defined the function $U_2(x)$:

$$U_2(x) = \frac{1}{2}x^2, \tag{2}$$

as the van der Pol energy potential, which represents a simple well (see Fig. 1 (a)). The potential has a minimum located at $x = 0$.

To express Equation (1) as a dynamical system and to analyze the fixed points, we set $\dot{x} = u$ and drop the forcing to obtain

$$\begin{aligned} \dot{x} &= u, \\ \dot{u} &= \mu(1-x^2)\dot{x} - x. \end{aligned} \quad (3)$$

We can observe from Equation (3) that the only fixed point is located at $(x = 0, u = 0)$. For the case when $A_2 = 0$ the van der Pol system satisfies the Lienard theorem, giving a limit cycle in the phase space, around the origin.

On the other hand, the Duffing oscillator is a nonlinear dynamical system governed by

$$\ddot{y} + \alpha\dot{y} + \frac{dU_1(y)}{dy} = A_1 \cos(\omega_1 t), \quad (4)$$

where

$$U_1(y) = -\frac{1}{2}y^2 + \frac{1}{4}\varepsilon y^4, \quad (5)$$

and α is positive and it denotes a dissipative parameter, ε is a positive constant that controls the nonlinearity of the system, and A_1 is the amplitude of the external forcing, being ω_1 its frequency. The potential in Equation (5) represents a double well shown in Fig. 1 (b). The local minima of this potential are in $y = \pm\frac{1}{\sqrt{\varepsilon}}$ and the local maximum is located at $y = 0$. As a dynamical system the Duffing Equation in (4) (no forcing) can be cast as

$$\begin{aligned} \dot{y} &= v, \\ \dot{v} &= -\alpha v + y - \varepsilon y^3. \end{aligned} \quad (6)$$

Here, we set $\dot{y} = v$. The fixed points for these systems are in the phase space at $(y = 0, v = 0)$ and $\left(y = \pm\frac{1}{\sqrt{\varepsilon}}, v = 0\right)$. The first point at $(y = 0, v = 0)$ is a saddle point, while the others, depending on the parameter α, they can be stable or unstable points. For $\alpha > 0$ the points result stables, for the $\alpha = 0$ case, the resulting dynamics is of type center and for $\alpha < 0$ case, the points result unstable. When the damping is positive $(\alpha > 0)$, the trajectory of the system is stable spiral conversely, for a damping negative $(\alpha < 0)$, the trajectory is unstable spiral at the fixed points $\left(y = \pm\frac{1}{\sqrt{\varepsilon}}, v = 0\right)$ in both cases.

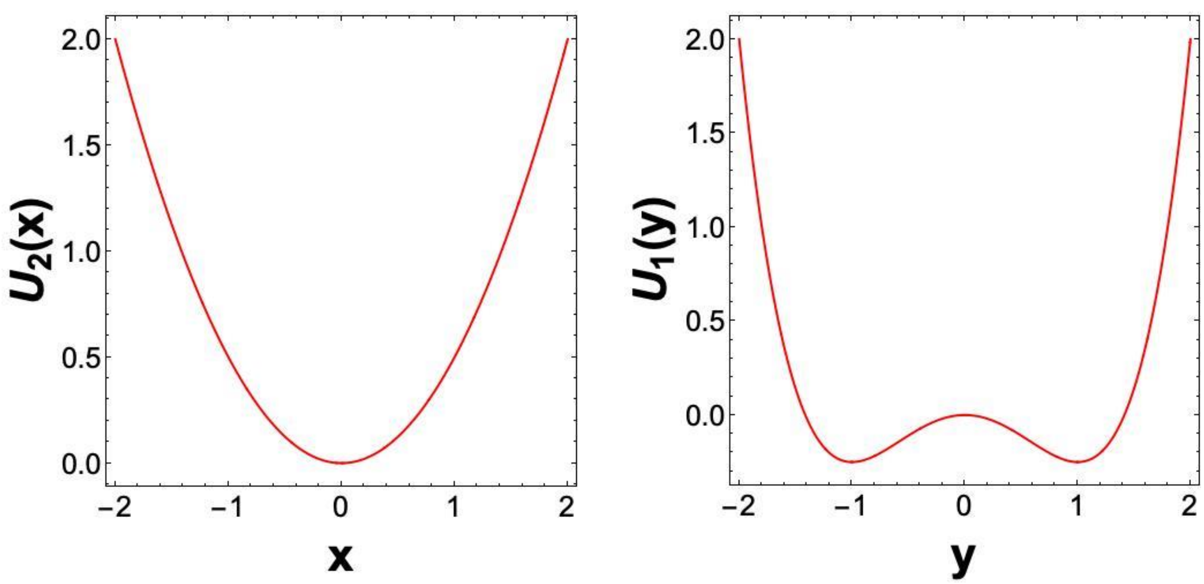

a) b)

Figure 1. The potentials $U_2(x)$ and $U_1(y)$. (a) The potential corresponds to the van der Pol oscillator. (b) The Duffing oscillator $(\varepsilon = 1)$.

3. Master-slave synchronization

In this section, three different couplings for the van der Pol and Duffing systems are studied and compared among themselves, namely: the elastic, the dissipative and the one that combines elastic and dissipative couplings employed by Uriostegui-Legorreta et al. (2021). Let us stress that most of the research on synchronization is based on autonomous systems of three dimensions or higher Boccaletti et al. (2002), Pecora and Carroll (2015), Zhang et al. (2009). Three of the most studied nonautonomous systems of low-dimensionality with forcing are the Duffing, van der Pol, Rayleigh and their variations, since much of the dynamical features embedded in the physical systems can be realized on these systems Chang (2017), Siewe et al. (2010b), Wang and Li (2015). One important implication is that a two-dimensional continuous dynamical system cannot give rise to strange attractors. In particular, chaotic behavior arises only in continuous dynamical systems of three dimensions or higher. Most of the research on synchronization is based on autonomous systems that satisfy the Poincaré-Bendixson theorem. Nevertheless, let us stress that the van der Pol and Duffing oscillators being of two-dimensional, need an external forcing to present chaos. In general, the synchronization problem reduces to finding a suitable value of the coupling strength G, (denoted by G^*) being in the range $G \geq G^* > 0$, such that the master and slave systems synchronize. Thus, for a coupling strength G^*, when the complete synchronization is reached, the error function goes to zero:

$$\lim_{t\to\infty}|y(t)-x(t)| = \lim_{t\to\infty}|v(t)-u(t)| = 0. \tag{7}$$

When the system is in practical synchronization, for a certain value of G^*, the error functions satisfy

$$\lim_{t\to\infty}|y(t)-x(t)| \leq \delta, \tag{8}$$

$$\lim_{t\to\infty}|v(t)-u(t)| \leq \tau, \tag{9}$$

for given positive values δ, $\tau > 0$ and arbitrary initial conditions. This definition is used, because, sometimes, the errors do not exactly converge to zero, but in practice we still can speak of synchronized systems. In some cases, it can be reached complete synchronization in a single state of the system while in the other, it can be only obtained practical or null synchronization. Partial synchronization is the phenomenon when, in a dynamical system, only part of the state variables synchronize and the others do not do.

The dynamics for each oscillator under study is described by the Equations (1) and (4). The values of the parameters we use are as follows: $\mu = 0.8$, $\alpha = 0.3$, $\varepsilon = 1$, $A_1 = 0.5$, $\omega_1 = 1.3$, $A_2 = 0.6$ and $\omega_2 = 0.4$. In Fig. 2 it is displayed the respective trajectories with the initial conditions $x(0) = 0.8$, $y(0) = 2$, $u(0) = 1$ and $v(0) = 0.5$. Let us mention that the very same values of the parameters and the initial conditions will be used in the subsequent numerical simulations. The numerical simulations were achieved using the fourth order of the Runge–Kutta method.

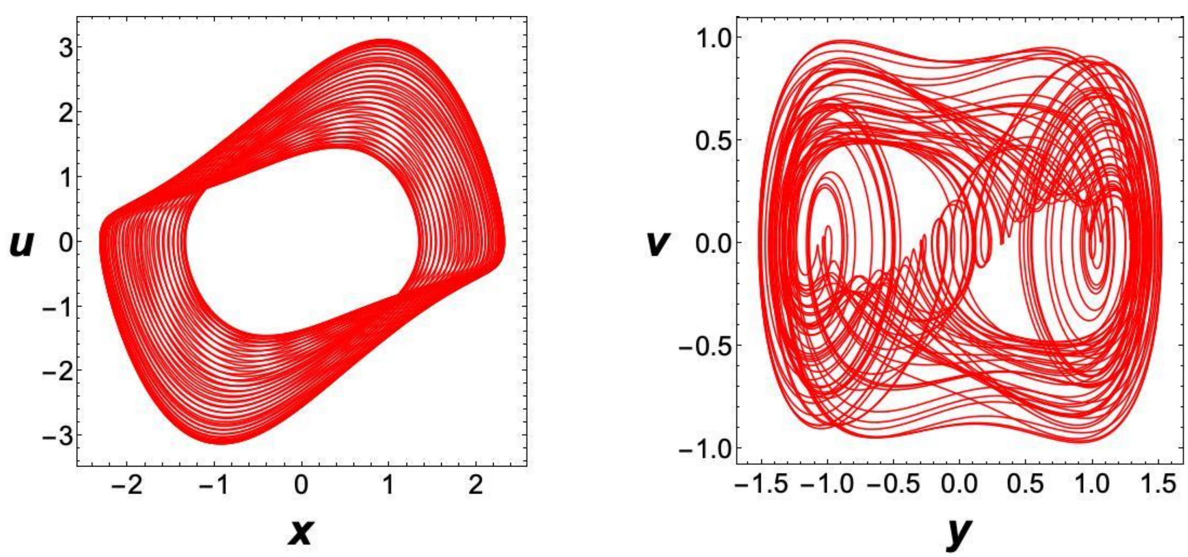

a) b)

Figure 2. In (a) van der Pol oscillator described by Eq. (1). In (b) Duffing oscillator described by Eq. (4).

A modified master-slave scheme leading to synchronization even in the cases where the classical master-slave scheme fails, was considered by Uriostegui-Legorreta et al. (2021). The system analyzed in this reference can be separated into two parts (see Equations 10 and 11). In one side, the system combines a non-conventional coupling, where a linear feedback is made. The elastic coupling is proportional to the difference of the position, $G_1(y-x)$, which is introduced in the velocity of the slave system. The other part also uses another linear feedback proportional to the difference of the velocity (dissipative coupling), $G_2(y-x)$, introduced in the acceleration in the slave system. For the van der Pol and Duffing oscillators, the equations that govern the evolution are

$$Master: \begin{cases} \dot{y} = v, \\ \dot{v} = -\alpha v + y - \varepsilon y^3 + A_1 \cos(\omega_1 t), \end{cases} \tag{10}$$

$$Slave: \begin{cases} \dot{x} = u + G_1(y-x), \\ \dot{u} = \mu(1-x^2)u - x + A_2 \cos(\omega_2 t) + G_2(v-u). \end{cases} \tag{11}$$

The errors $e_1 = y - x$ and $e_2 = v - u$, are determined by subtracting Equations (10) and (11), giving

$$\begin{aligned} \dot{e}_1 &= \dot{y} - \dot{x} = v - u - G_1 e_2, \\ e_2 &= v - u = \dot{e}_1 + G_1 e_1, \\ \dot{e}_2 &= \dot{v} - \dot{u} = -\alpha v + y - \varepsilon y^3 + A_1 \cos(\omega_1 t) \\ &\quad -\mu(1-x^2)u + x - A_2 \cos(\omega_2 t) - G_2 e_2. \end{aligned} \tag{12}$$

The constant G_1 corresponds to the elastic coupling and G_2 to the dissipative coupling. Hence, $G_1(y-x) = G_1(e_1)$ and $G_2(v-u) = G_2(\dot{e}_1 + G_1 e_1)$, which manifest the dependence of G_2 on the derivative of error and the coupling G_1, giving more information about the dynamical evolution of the system. For definiteness, let us express Equations (10) and (11) in matrix form for the case of two distinct couplings

$$\begin{pmatrix} \dot{y} \\ \dot{v} \end{pmatrix} = \begin{pmatrix} 0 & 1 \\ 1 & -\alpha \end{pmatrix} \begin{pmatrix} y \\ v \end{pmatrix} + \begin{pmatrix} 0 \\ -\varepsilon y^3 \end{pmatrix} + \begin{pmatrix} 0 \\ A_1 cos(\omega_1 t) \end{pmatrix}, \tag{13}$$

$$\begin{pmatrix} \dot{x} \\ \dot{u} \end{pmatrix} = \begin{pmatrix} 0 & 1 \\ -1 & \mu \end{pmatrix} \begin{pmatrix} x \\ u \end{pmatrix} + \begin{pmatrix} 0 \\ -\mu x^2 u \end{pmatrix} + \begin{pmatrix} 0 \\ A_2 cos(\omega_2 t) \end{pmatrix} + \begin{pmatrix} G_1 e_1 \\ G_2 \dot{e}_1 + G_1 G_2 e_1 \end{pmatrix}. \tag{14}$$

The first vectors in Equations (13) and (14) on the right-hand side contain the nonlinearity information of the system, while the second ones give the information on the external forcing. The last vector in (14) is the so-called control vector. Notice that the control depends on the error and its derivative. For the case $G_1 = G_2 = 0$ the system decouples. To study the dynamics of the system, we vary the couplings G_1 and G_2 keeping one of them constant, while the other is varied. Let us consider the $|y(t) - x(t)|$ and $|v(t) - u(t)|$ error functions. We calculate $|y(t) - x(t)|$ keeping $G_2 = 100$ and varying G_1 in small steps from 0 to 10 with a time interval from 5000 to 6000. This time interval will be used in the calculations of the error functions for the three couplings used in this work. In a similar way, we obtain the error function $|v(t) - u(t)|$ with $G_1 = 5$ and varying G_2 in small steps from 0 to 200. As it can be appreciated from Figs. 3 (a) and (b), we obtain complete synchronization, since the error functions go to zero as the value of G_1 and G_2 are increased. The plots of $|e_1|$ and $|e_2|$ as a function of t, for the values of $G_1 = 5$ and $G_2 = 100$, are depicted in Fig. 4.

Let us now analyze the projections onto the (x, y) and (u, v) planes for values of $G_1 = 5$ and $G_2 = 100$. For this case, the Duffing oscillator is in a chaotic regime; the van der Pol oscillator is maintained as the slave system. In Figs. 5 (a) and (b) the behavior of the Duffing and van der Pol oscillators is shown, respectively, while in (c) and (d), it can be observed that complete synchronization is reached for these systems.

For the configuration master-slave, in which the Duffing oscillator acts as master and the van der Pol as slave, we will analyze the elastic coupling. For this case, we have

$$Master: \begin{cases} \dot{y} = v, \\ \dot{v} = -\alpha v + y - \varepsilon y^3 + A_1 \cos(\omega_1 t), \end{cases} \tag{15}$$

$$Slave: \begin{cases} \dot{x} = u, \\ \dot{u} = \mu(1-x^2)u - x + A_2 \cos(\omega_2 t) + K(y-x). \end{cases} \tag{16}$$

In this instance, the coupling is represented by $K(y-x)$, being K the coupling parameter to be varied. For the $K = 0$ case, the system decouples. The coupling is a lineal feedback to the slave oscillator proportional to the difference of the position. We are interested in studying how the dynamics of the system evolves as the constant coupling K is changed.

Let us consider again the error functions $|y(t) - x(t)|$ and $|v(t) - u(t)|$ by taking K as a control parameter to be varied in small steps from 0 to 200. For our case, the error functions allow us to find the range of values for K in which the synchronization is reached in the projections onto the (x, y) and (u, v) planes, as it can be shown in Figs. 6 (a) and (b). As it can be observed, no synchronization exists in this kind of coupling, since the error functions $|y(t) - x(t)|$ and $|v(t) - u(t)|$ do not vanish. In order to see this, let us observe that the errors $e_3 = y - x$ and $e_4 = v - u$ can be calculated from Equations (15) and (16) as:

$$\begin{aligned} \dot{e}_3 &= \dot{y} - \dot{x} = e_4, \\ \dot{e}_4 &= \dot{v} - \dot{u} = -\alpha v + y - \varepsilon y^3 + A_1 \cos(\omega_1 t) \\ &\quad -\mu(1-x^2)u + x - A_2 \cos(\omega_2 t) - K e_3. \end{aligned} \tag{17}$$

The plots of $|e_3|$ and $|e_4|$ as a function of t for a value of $K = 200$, are depicted in Fig. 7. To corroborate

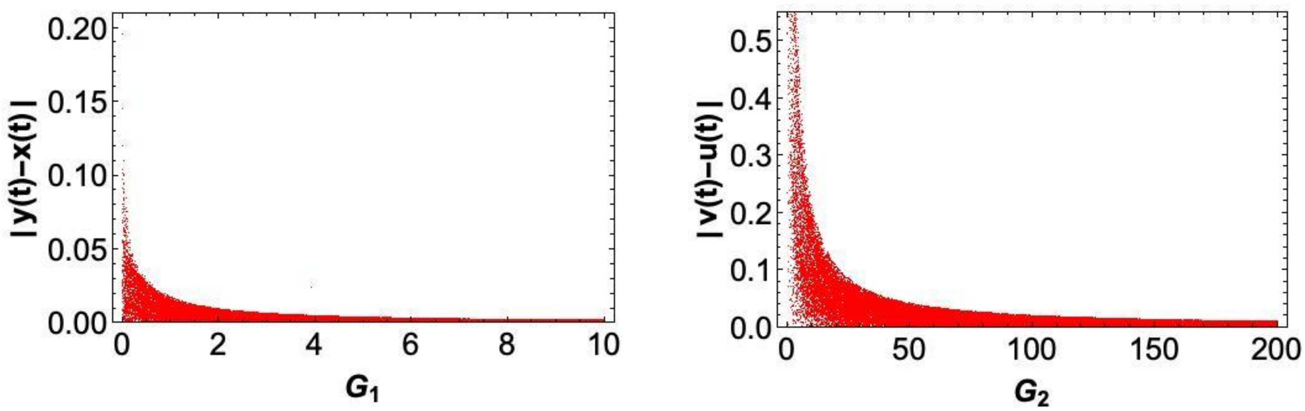

a) b)

Figure 3. The error functions varying the parameters couplings G_1 and G_2.
In (a) it is represented $|y(t) - x(t)|$, with $G_2 = 100$ and varying G_1. In (b) $|v(t) - u(t)|$, with $G_1 = 5$ and varying G_2.

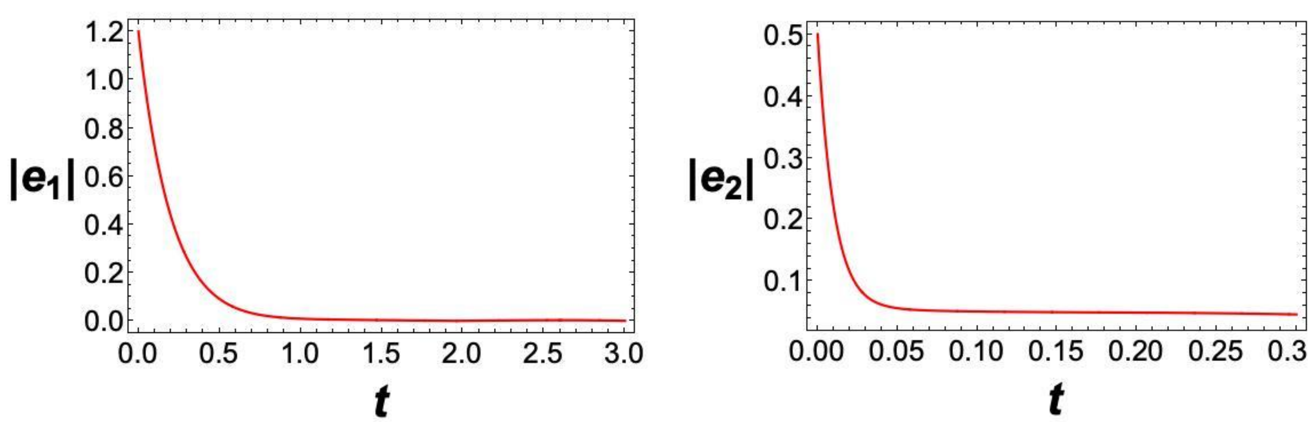

Figure 4. Error functions for $|e_1|$ and $|e_2|$ with respective values of $G_1 = 5$ and $G_2 = 100$.

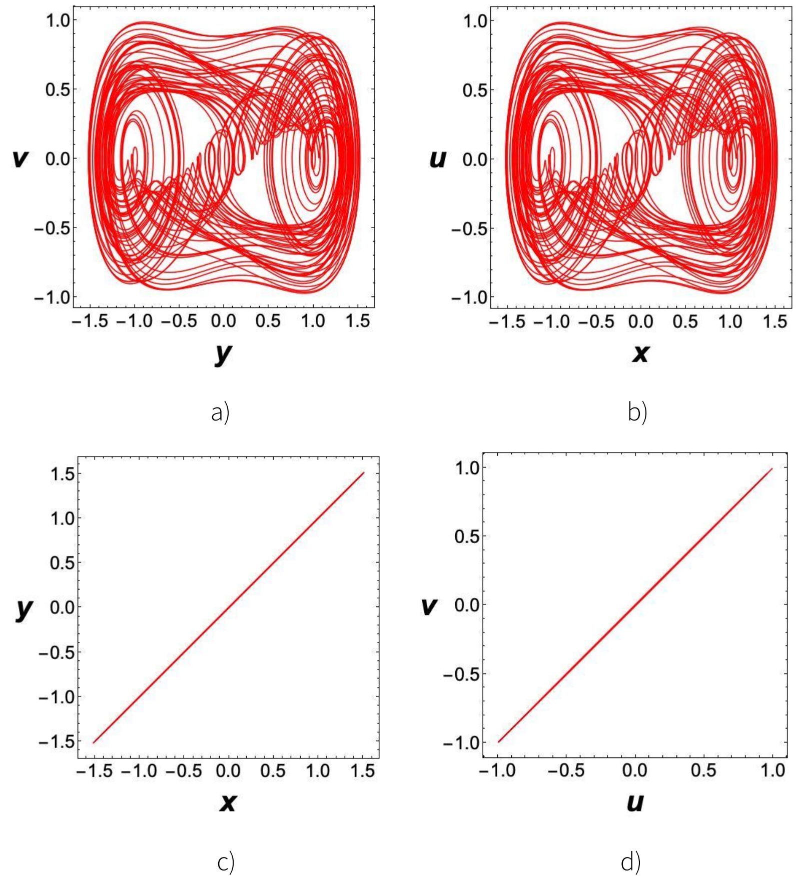

Figure 5. Elastic and dissipative couplings for $G_1 = 5$ and $G_2 = 100$.
In (a) the Duffing oscillator (master). In (b) the van der Pol oscillator (slave).
In (c) and (d) projections onto the (x, y) and (u, v) planes, respectively.

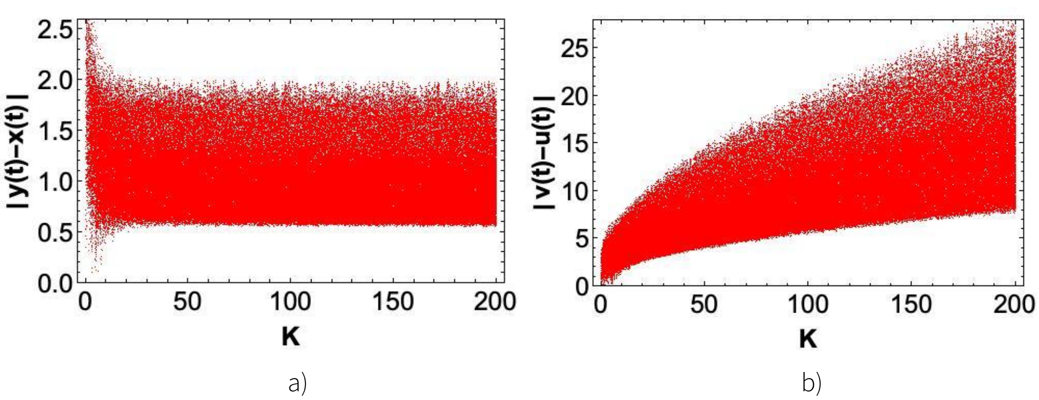

Figure 6. The error functions: In (a) represents $|y(t) - x(t)|$, and in (b) $|v(t) - u(t)|$, both as a function of the parameter K.

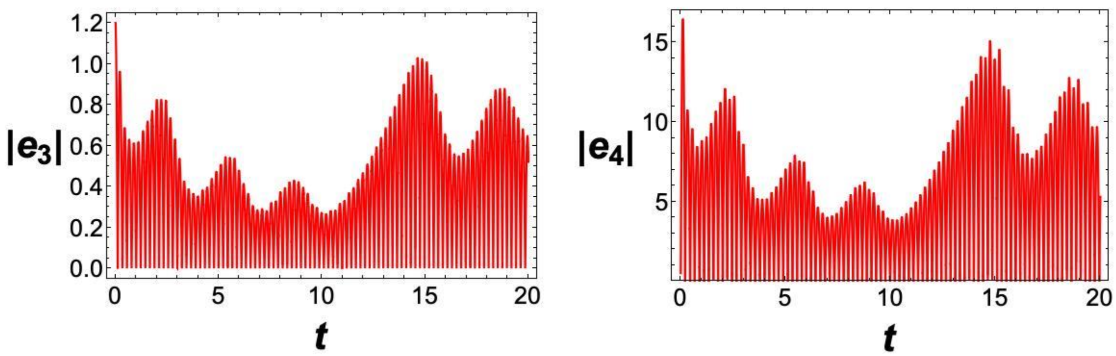

Figure 7. Error functions for $|e_3|$ and $|e_4|$ as a function of t, for a value of $K = 200$.

that no synchronization exists, let us analyze the projections onto the (x, y) and (u, v) planes for a particular value $K = 200$. For this case, the master system is working in the chaotic regime and the dynamics of the van der Pol oscillator is not being controlled by Duffing oscillator as it can be observed from Figs. 8 (a) and (b). In Figs. 8 (c) and (d) the projections onto the (x, y) and (u, v) planes no synchronization exists. If we have had synchronization, we could observe a straight line at $45°$ on both mentioned projections, but it is not the case. Let us mention that, regardless of the former conclusion, the elastic coupling is still used in bidirectional synchronization Kengne et al. (2012). Thus, it is important to discuss here this kind of coupling.

Let us now discuss the synchronization when the oscillators are coupled through a dissipative coupling, represented by

$$Master: \begin{cases} \dot{y} = v, \\ \dot{v} = -\alpha v + y - \varepsilon y^3 + A_1 \cos(\omega_1 t), \end{cases} \tag{18}$$

$$Slave: \begin{cases} \dot{x} = u, \\ \dot{u} = \mu(1 - x^2)u - x + A_2 \cos(\omega_2 t) + H(v - u). \end{cases} \tag{19}$$

Here $H(v - u)$ represents the dissipative coupling, being H used as a parameter. As before, for the $H = 0$ case, the oscillators become decoupled. The dissipative coupling is also a lineal feedback to the slave oscillator proportional to the difference of velocity.

As before, we consider the error functions, with H varied from 0 to 200 in small steps. These plots allow us to find the range of values for H in which the synchronization could be reached as it is shown in Figs. 9 (a) and (b). Notice that in the projection onto the (x, y) plane no synchronization exists since the error function $|y(t) - x(t)|$ results large; the $|v(t) - u(t)|$ function goes to zero for large values of H. For the projection onto the (u, v) plane, the complete synchronization could be reached for large values of H. For the dissipative coupling, the errors $e_5 = y - x$ and $e_6 = v - u$, are determined by subtracting Equations (18) and (19), given

$$\begin{aligned} \dot{e}_5 &= \dot{y} - \dot{x} = e_6, \\ \dot{e}_6 &= \dot{v} - \dot{u} = -\alpha v + y - \varepsilon y^3 + A_1 \cos(\omega_1 t) \\ &\quad -\mu(1 - x^2)u + x - A_2 \cos(\omega_2 t) - H\dot{e}_5. \end{aligned} \tag{20}$$

The plots of $|e_5|$ and $|6|$ as a function of t for a value of $H = 200$, are depicted in Fig. 10.

Let us analyze the projections onto the (x, y) and (u, v) planes for a specific value of $H = 200$. In this case the master system is in a chaotic regime. In Fig. 11 (a) it is shown the Duffing oscillator (master system) while in Fig. 11 (b) it is represented the van der Pol oscillator (slave system). In Fig. 11 (c) we can appreciate the fact that in the projection onto the (x, y) plane there is no synchronization while in the projection onto the (u, v) plane there is only complete synchronization (Fig. 11 (d)).

For certain systems, it is not possible to reach synchronization when the classical master-slave scheme is used. Specifically, there are cases where it is impossible to find a coupling constant K such that the systems reach synchronization, as it occurs for the systems described by Equation (15) and (16). In some cases, the systems reach complete synchronization in a single state of the slave system as it occurs for the dynamics contained in Equations (18) and (19), depending of the value H. Variations to the master-slave scheme for some systems have been proposed to solve certain kind of problems Aydogmus and Tosyali (2022), Buscarino et al. (2019), Ding (2019), Ramirez et al. (2020). In particular, Uriostegui-Legorreta et al. (2021) a modified master-slave scheme is considered that leads to synchronization even in the cases where the classical master-slave scheme fails.

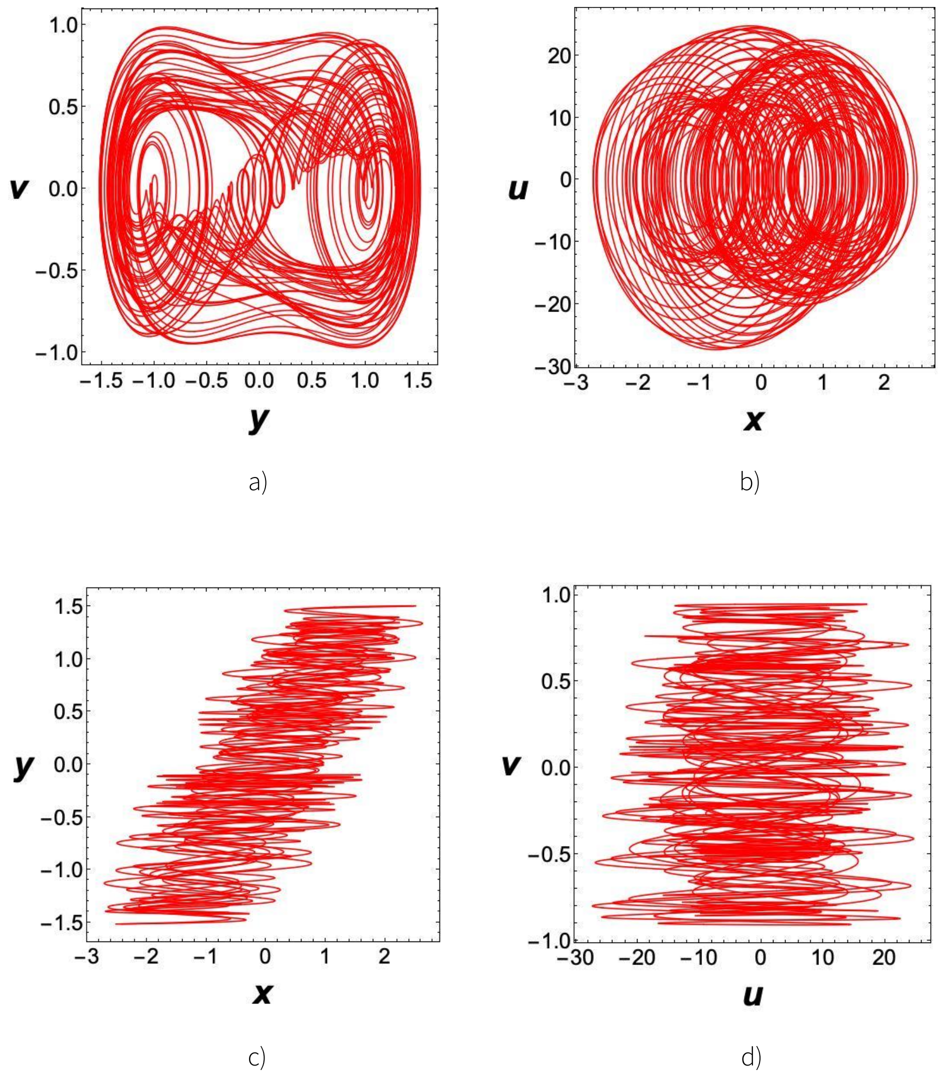

Figure 8. Elastic coupling, for a parameter control of $K = 200$. In (a) the Duffing oscillator.
In (b) the van der Pol oscillator. In (c) and (d) projections onto the (x, y) and (u, v) planes respectively.

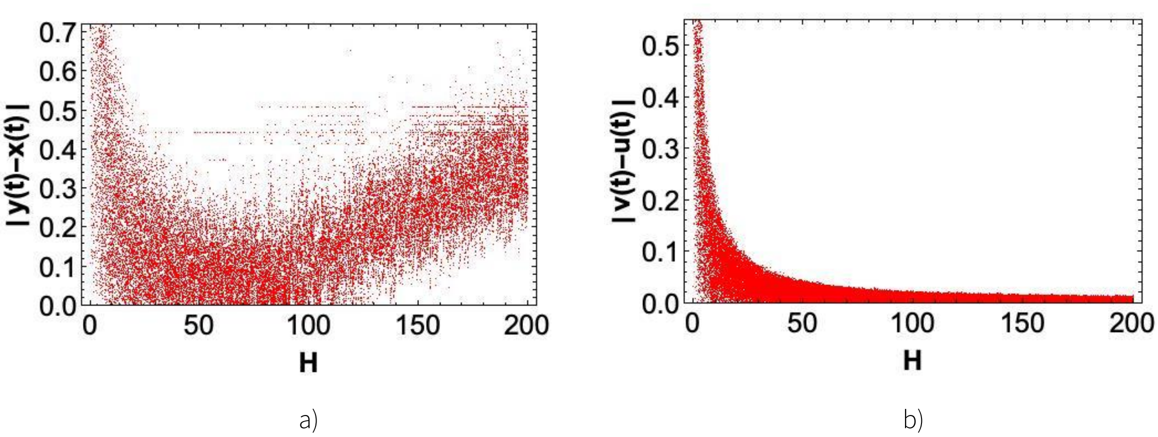

Figure 9. The error functions: In (a) represents $|y(t) - x(t)|$, and in (b) $|v(t) - u(t)|$,
both as a function of the parameter H.

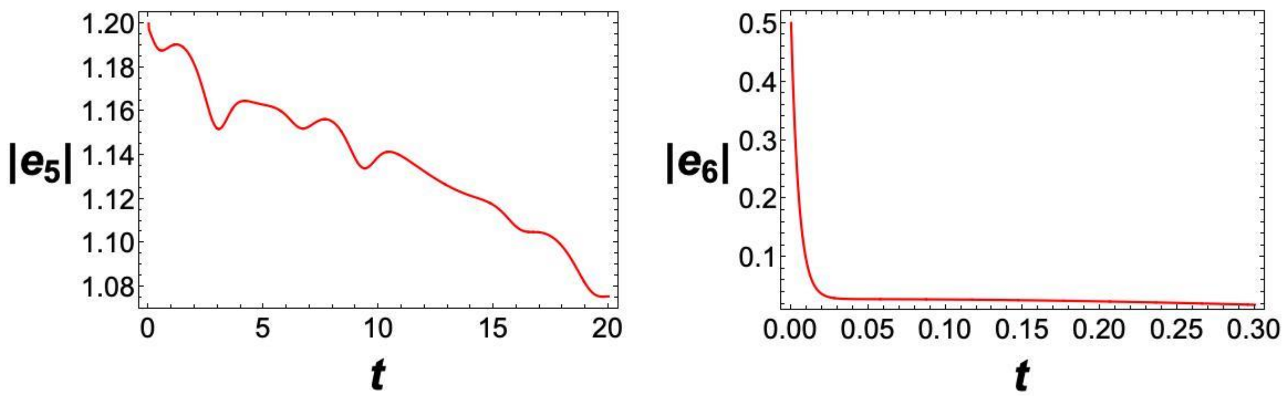

Figure 10. Error functions $|e_5|$ and $|6|$, for $H = 200$.

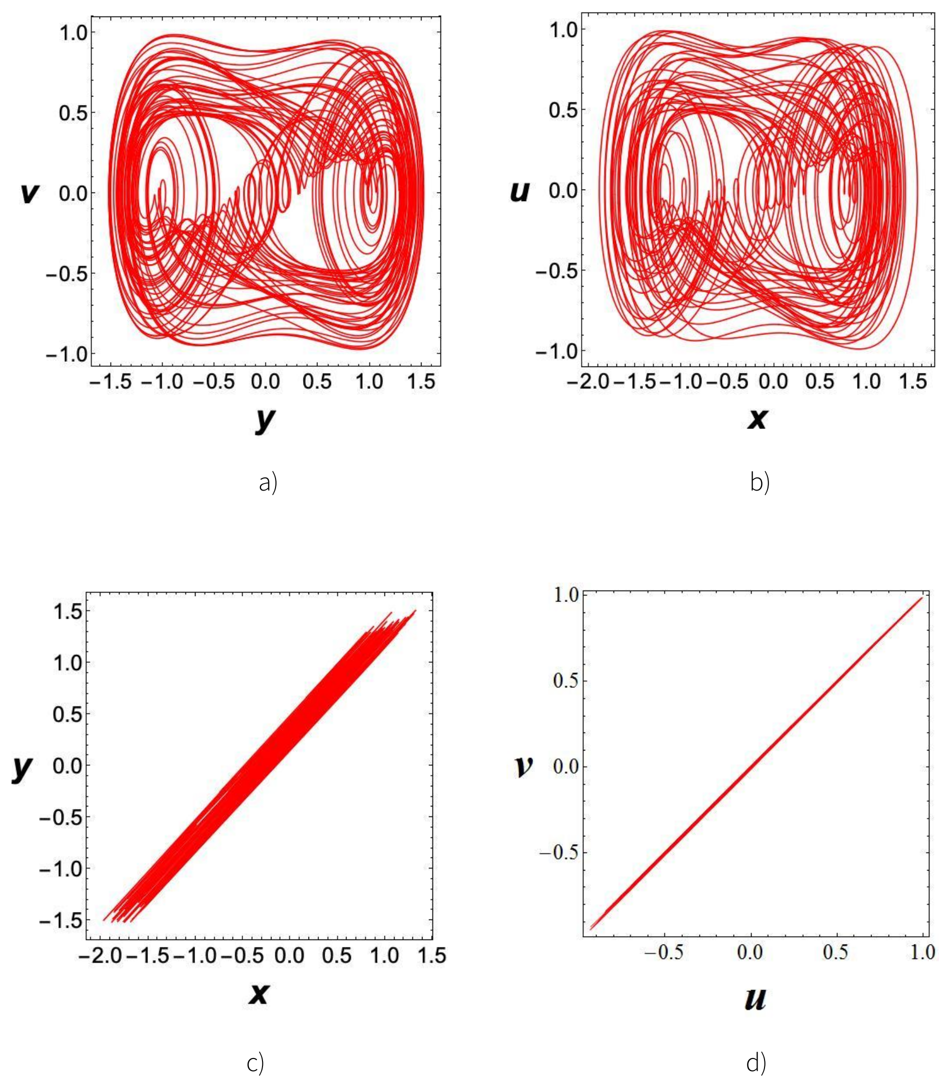

Figure 11. Dissipative coupling case, for $H = 200$. In (a) the Duffing oscillator (master) and in (b) the van der Pol oscillator (slave). In (c) and (d) projections onto the (x, y) and (u, v) planes, respectively.

4. Conclusions

The van der Pol and Duffing are low-dimensionality nonautonomous systems that present chaos and have been well studied. One of the conclusions presented in the literature is that the classical master-slave configuration (by using elastic coupling), for the van der Pol and Duffing oscillators, does not offer synchronization. In this work, we have shown that for this same coupling, in master-slave configuration and when the dissipative coupling is used, only complete synchronization in the projection onto the (u, v) plane can be reached. In fact, according to the classical master-slave configuration in the best of cases, it is obtained only complete synchronization in a single state of the slave system studied. On the other hand, the possibility of using two coupling (elastic and dissipative, in this case), blending up as one, allows the system more interesting dynamics and a broad range for the control parameters. In this paper, we have analyzed the synchronization in the van der Pol and Duffing oscillators using the blending of the elastic and dissipative couplings. We observed that, in a difference with other approaches, with this new coupling, we were able of obtaining complete synchronization in the projections onto the (x, y) and (u, v) planes. In order to apply synchronization in communication systems, it is necessary to have a large range of the control parameters, which is obtained in the van der Pol and Duffing oscillators, by employing our approach of coupling. This kind of coupling will be applied in other systems that do not present synchronization through the usual methods.

Conflict of interest

The authors do not have any type of conflict of interest to declare.

Acknowledgments

This work has been partially supported by UMNSH. U. Uriostegui-Legorreta thanks to CONACYT for financial support.

Financing

U. Uriostegui-Legorreta acknowledges financial support by CONACYT, Grant No. 2001921.

References

Anzo-Hernández, A., Campos-Cantón, E., & Nicol, M. (2019). Itinerary synchronization between PWL systems coupled with unidirectional links. *Communications in Nonlinear Science and Numerical Simulation*, *70*, 102-124. https://doi.org/10.1016/j.cnsns.2018.10.020

Aydogmus, F., & Tosyali, E. (2022). Master–slave synchronization in a 4D dissipative nonlinear fermionic system. *International Journal of Control*, *95*(3), 620-625. https://doi.org/10.1080/00207179.2020.1808244

Boccaletti, S., Kurths, J., Osipov, G., Valladares, D. L., & Zhou, C. S. (2002). The synchronization of chaotic systems. *Physics reports*, 366(1-2), 1-101. https://doi.org/10.1016/S0370-1573(02)00137-0

Buscarino, A., Fortuna, L., & Patanè, L. (2019). Master-slave synchronization of hyperchaotic systems through a linear dynamic coupling. *Physical Review E*, *100*(3), 032215. https://doi.org/10.1103/PhysRevE.100.032215

Campos, E., Urías, J., & Rulkov, N.F. (2004). Multimodal synchronization of chaos. Chaos: *An Interdisciplinary Journal of Nonlinear Science*, 14(1), 48-54. https://doi.org/10.1063/1.1624651

Chaharborj, S.C., Chaharborj. S.C., & See, P.P. (2021). Application of Chebyshev neural network to solve Van der Pol equations. *International Journal of Basic and Applied Sciences*, *10*(1), 7-19. https://doi.org/10.14419/ijbas.v10i1.31431

Chang, T. P. (2017). Chaotic motion in forced duffing system subject to linear and nonlinear damping. *Mathematical Problems in Engineering*, Vol. 2017, 3769870. https://doi.org/10.1155/2017/3769870

Chedjou, J. C., Fotsin, H. B., Woafo, P., & Domngang, S. (2001). Analog simulation of the dynamics of a van der Pol oscillator coupled to a Duffing oscillator. *IEEE Transactions on Circuits and Systems I: Fundamental Theory and Applications*, *48*(6), 748-757. https://doi.org/10.1109/81.928157

Chedjou, J. C., Kyamakya, K., Moussa, I., Kuchenbecker, H. P., & Mathis, W. (2006). Behavior of a Self-Sustained Electromechanical Transducer and Routes to Chaos. *128*(3), 282-293.
https://doi.org/10.1115/1.2172255

Chekan, J.A., Nojoumian, M.A., Merat, K., & Salarieh, H. (2017). Chaos control in lateral oscillations of spinning disk via linear optimal control of discrete systems. *Journal of Vibration and Control*, *23*(1), 103-110.
https://doi.org/10.1177/1077546315575248

Chua, L.O., Itoh, M., Kocarev, L., & Eckert, K. (1993). Chaos Synchronization in Chua´s Circuit. *Journal of Circuits, Systems and Computers*, *3*(01), 93-108.
https://doi.org/10.1142/S0218126693000071

Ding, K. (2019). Master-Slave Synchronization of Chaotic Φ^6 Duffing Oscillators by Linear State Error Feedback Control. *Complexity*, Vol. 2019, 3637902.
https://doi.org/10.1155/2019/3637902

Ding, M., & Yang, W. (1996). Observation of intermingled basins in coupled oscillators exhibiting synchronized chaos. *Physical Review E*, *54*(3), 2489.
https://doi.org/10.1103/PhysRevE.54.2489

Dongmo, E.D., Ojo, K.S., Woafo, P., & Njah, A.N. (2018). Difference Synchronization of Identical and Nonidentical Chaotic and Hyperchaotic Systems of Different Orders Using Active Backstepping Design. *Journal of Computational and Nonlinear Dynamics*, *13*(5), 051005.
https://doi.org/10.1115/1.4039626

Dutra, M.S., de Pina Filho, A.C., & Romano, V.F. (2003). Modeling of a bipedal locomotor using coupled nonlinear oscillators of Van der Pol. *Biological Cybernetics*, *88(*4), 286-292.
https://doi.org/10.1007/s00422-002-0380-8

González Salas, J.S., Campos Cantón, E., Ordaz Salazar, F.C., & Campos Cantón, I. (2008). Forced synchronization of a self-sustained chaotic oscillator. Chaos: *An Interdisciplinary Journal of Nonlinear Science*, *18*(2), 023136.
https://doi.org/10.1063/1.2947661

Huang, C., & Cao, J. (2017). Active control strategy for synchronization and anti-synchronization of a fractional chaotic financial system. Physica A: *Statistical Mechanics and Its Applications*, *473*, 262-275.
https://doi.org/10.1016/j.physa.2017.01.009

Jasni, F., & Shafie, A. A. (2012). Van Der Pol central pattern generator (VDP-CPG) model for quadruped robot. In *Trends in Intelligent Robotics, Automation, and Manufacturing: First International Conference, IRAM 2012, Kuala Lumpur, Malaysia, November 28-30, 2012. Proceedings* (pp. 167-175). Springer Berlin Heidelberg.
https://doi.org/10.1007/978-3-642-35197-6_18

Kengne, J., Chedjou, J.C., Kenne, G., Kyamakya, K., & Kom, G.H. (2012). Analog circuit implementation and synchronization of a system consisting of a van der Pol oscillator linearly coupled to a Duffing oscillator. *Nonlinear Dyn*, *70*, 2163-2173.
https://doi.org/10.1007/s11071-012-0607-8

Kengne, J., Kenmogne, J., & Kamdoum, J. (2014). Experiment on bifurcation and chaos in coupled anisochronous self-excited systems: Case of two coupled van der Pol-Duffing oscillators. *Journal of Nonlinear Dynamics*, *2014*, 815783.
https://doi.org/10.1155/2014/815783

Khan, A. (2017). Hybrid function projective synchronization of chaotic systems via adaptive control. *International Journal of Dynamics and Control*, *5*(4), 1114-1121.
https://doi.org/10.1007/s40435-016-0258-6

Kuznetsov, A.P., & Roman, J.P. (2009). Properties of synchronization in the systems of non-identical coupled van der Pol and van der Pol–Duffing oscillators. Broadband synchronization. *Physica D: Nonlinear Phenomena*, *238*(16), 1499-1506.
https://doi.org/10.1016/j.physd.2009.04.016

Kuznetsov, A.P., Stankevich, N.V., & Turukina, L.V. (2009). Coupled van der Pol-Duffing oscillators: Phase dynamics and structure of synchronization tongues. *Physica D: Nonlinear Phenomena*, *238*(14), 1203-1215.
https://doi.org/10.1016/j.physd.2009.04.001

Lee, K. J., Kwak, Y., & Lim, T. K. (1998). Phase jumps near a phase synchronization transition in systems of two coupled chaotic oscillators. *Physical review letters*, *81*(2), 321.
https://doi.org/10.1103/PhysRevLett.81.321

López-Mancilla, D., López-Cahuich, G., Posadas-Castillo, C., Castañeda, C.E., García-López, J.H., Vázquez-Gutiérrez, J.L., & Tlelo-Cuautle, E. (2019). Synchronization of complex networks of identical and nonidentical chaotic systems via model-matching control. *PLOS ONE*, *14*(5), e0216349.
https://doi.org/10.1371/journal.pone.0216349

Lü, L., Zhang, F., & Han, C. (2019). Synchronization transmission of the target signal in the circuit network based on coupling technique. *Physica A: Statistical Mechanics and Its Applications*, *535*, 122412.
https://doi.org/10.1016/j.physa.2019.122412

Mall, S., & Chakraverty, S. (2016). Hermite Functional Link Neural Network for Solving the Van der Pol-Duffing Oscillator Equation. *Neural Computation*, *28*(8), 1574-1598.
https://doi.org/10.1162/NECO_a_00858

Murali, K., & Lakshmanan, M. (1993). Transmission of signals by synchronization in a chaotic Van der Pol–Duffing oscillator. *Physical Review E*, *48*(3), R1624.
https://doi.org/10.1103/PhysRevE.48.R1624

Njah, A.N. (2010). Synchronization via active control of parametrically and externally excited Φ^6 Van der Pol and Duffing oscillators and application to secure communications. *Journal of Vibration and Control*, *17*(4), 493-504.
https://doi.org/10.1177/1077546309357024

Ouannas, A., Azar, A. T., & Vaidyanathan, S. (2017). New hybrid synchronisation schemes based on coexistence of various types of synchronisation between master-slave hyperchaotic systems. *International Journal of Computer Applications in Technology*, *55*(2), 112-120.
https://doi.org/10.1504/IJCAT.2017.10003542

Pai, M. C. (2020). Sliding mode control for discrete-time chaotic systems with input nonlinearity. *Journal of Dynamic Systems, Measurement, and Control*, *142*(10), 101003.
https://doi.org/10.1115/1.4047218

Pastor-Díaz, I., & López-Fraguas, A. (1995). Dynamics of two coupled van der Pol oscillators. *Physical Review E*, *52*(2), 1480-1489.
https://doi.org/10.1103/PhysRevE.52.1480

Pecora, L. M., & Carroll, T. L. (1990). Synchronization in chaotic systems. *Physical review letters*. *64*(8), 821-824.
https://doi.org/10.1103/PhysRevLett.64.821

Pecora, L. M., & Carroll, L. M. (2015). Synchronization of chaotic systems. *Chaos*, *25*(9), 097611.
https://doi.org/10.1063/1.4917383

Razminia, A., & Dumitru, B. (2013). Complete synchronization of commensurate fractional order chaotic systems using sliding mode control. *Mechatronics*, *23*(7), 873-879.
https://doi.org/10.1016/j.mechatronics.2013.02.004

Ramirez, J.P., Garcia, E., & Alvarez, J. (2020). Master-slave synchronization via control dynamic control. *Commun Nonlinear Sci Numer Simulat*, *80*, 104977.
https://doi.org/10.1016/j.cnsns.2019.104977

Reick, C., & Mosekilde, E. (1995). Emergence of quasiperiodicity in symmetrically coupled, identical period-doubling systems. *Physical Review E*, *52*(2), 1418.
https://doi.org/10.1103/PhysRevE.52.1418

Siewe, S.M., Yamgoué, S.B., Moukam Kakmeni, F.M., & Tchawoua, C. (2010a). Chaos controlling self-sustained electromechanical seismograph system based on the Melnikov theory. *Nonlinear Dyn*, *62*, 379-389.
https://doi.org/10.1007/s11071-010-9725-3

Siewe, S.M., Tchawoua, C., & Woafo, P. (2010b). Melnikov chaos in a periodically driven Rayleigh-Duffing oscillator. *Mechanics Research Communications*, *37*(4), 363-368.
https://doi.org/10.1016/j.mechrescom.2010.04.001

Uriostegui-Legorreta, U., Tututi, E. S., & Arroyo-Correa, G. (2021). A new scheme of coupling and synchronizing low-dimensional dynamical systems. *Revista mexicana de física*, *67*(2), 334-342.
https://doi.org/10.31349/RevMexFis.67.334

Vincent, U. E., & Kenfack, A. (2008). Synchronization and bifurcation structures in coupled periodically forced non-identical Duffing oscillators. *Physica Scripta*, *77*(4), 045005.
https://doi.org/10.1088/0031-8949/77/04/045005

Wang, Y-Z., & Li, F-M. (2015). Dynamical properties of Duffing-van der Pol oscillator subject to both external and parametric excitations with time delayed feedback control. *Journal of Vibration and Control*, *21*(2), 371-387.
https://doi.org/10.1177/1077546313483160

Yan, J., & Li, C. (2005). Generalized projective synchronization of a unified chaotic system. Chaos, *Solitons & Fractals*, *26*(4), 1119-1124.
https://doi.org/10.1016/j.chaos.2005.02.034

Ye, Q., Jiang, Z., & Chen, T. (2018). Adaptive Feedback Control for Synchronization of Chaotic Neural Systems with Parameter Mismatches. *Complexity*, *2018*, 5431987.
https://doi.org/10.1155/2018/5431987

Yin, H. W., Dai, J. H., & Zhang, H. J. (1998). Phase effect of two coupled periodically driven Duffing oscillators. *Physical Review E*, *58*(5), 5683.
https://doi.org/10.1103/PhysRevE.58.5683

Zhang, H., Liu, D., & Wang, Z. (2009). *Controlling chaos: suppression, synchronization and chaotification*. Springer Science & Business Media.
https://doi.org/10.1007/978-1-84882-523-9